Joint Motion Capture and Navigation in Heterogeneous Body Area Networks with Distance Estimation Over Neighborhood Graph

Jihad Hamie, Benoît Denis
CEA-Leti Minatec Campus
17 rue des Martyrs, 38054 Cedex 09
Grenoble, France
Email: [jihad.hamie, benoit.denis]@cea.fr

Cedric Richard
Université de Nice Sophia-Antipolis / UMR CNRS 6525
Parc Valrose, 06108 Cedex 2
Nice, France
Email: cedric.richard@unice.fr

***Abstract*—We present and compare here solutions adapted to heterogeneous *Wireless Body Area Networks* (WBANs) to jointly fulfil indoor navigation and motion capture needs over large-scale trajectories. On-body devices are localized at the building scale by combining peer-to-peer range measurements over intra-WBAN links and further measurements with respect to external anchors forming the building infrastructure. Those measurements rely on two main low data rate radio technologies, namely the *Impulse Radio - Ultra Wideband* (IR-UWB) and a *Narrow Band* technology at 2.4GHz, providing respectively *Time (Difference) Of Arrival* (T(D)OA) estimates and *Received Signal Strength Indicators* (RSSI). This new *Large Scale Individual Motion Capture* (LSIMC) functionality is then investigated within two algorithmic embodiments. In a first 2-step scheme, the positions of on-body nodes are preliminary estimated in a body-strapped *Local Coordinates System* (LCS) before being expressed into an absolute *Global Coordinates System* (GCS) after a set of transformations, whereas the second option considers localizing directly the nodes into the GCS using all the available measurements. Simulations illustrate particularly the harmful impact of body obstructions. We also propose a method to mitigate these effects and approximate measurements over obstructed or erroneous links, by computing the shortest distance in graph neighborhood.**

I. Introduction

Motion capture applications relying on wearable sensors or tags have been considered so far in both stand-alone or infrastructure-based system architectures, with various technologies such as video acquisition [1], [2], magnetic fields sensing [3], inertial devices [4], [5] or even the fusion of different modalities [6], [7]. Such on-body sensors are most often interconnected to form *Wireless Body Area Networks* (WBAN) in order to communicate their measurement data to a collector or a gateway. Video systems are rather precise but they must operate in geographically restricted (i.e. limited by the coverage of the deployed cameras) and opened (i.e. obstruction-free) areas. Accordingly they can hardly work in non-controlled indoor environments over large-scale body movements. Magnetic field sensing is traditionally subject to disturbances due to the presence of metallic pieces in the vicinity of on-body sensors (e.g. embedded in clothes or in pieces of furniture). As for inertial solutions based on accelerometers and/or gyroscopes, they are usually affected by significant drifts over time.

As an alternative to the previous techniques, stand-alone wireless solutions have also been investigated recently, making direct and opportunistic use of the transmitted radio packets in WBANs under arbitrary nodes deployment. They rely on cooperative peer-to-peer range measurements through e.g., *Time Of Arrival* (TOA) estimation over *Impulse Radio - Ultra Wideband* (IR-UWB) links [8]-[11] or even *Received Signal Strength Indicators* (RSSI) over narrowband links [12]. Unfortunately, the latter solutions can mostly provide relative localization, but not yet absolute positioning of the on-body nodes at the building scale. Moreover, they still suffer from rather low accuracy, due to body shadowing and partial connectivity under pedestrian mobility, as well as poor relative ranging precision at the body scale.

But stand-alone radio-based [13] or inertial-aided [14] indoor navigation has also been intensively studied for years. However, in practical operating conditions (i.e. with a radio device hold in the user's hand or in the pocket), experiments prove that propagation phenomena can play a harmful role on the final localization performance. Radio obstructions or unfavorable device attitudes can indeed lead to significant errors on measured distances and hence, ultimately on position estimates. Strong limitations are for instance due to dense multipath, *Non-Line of Sight* (NLOS) wall obstructions and body shadowing, small-scale fading or radio irregularities (e.g. non-calibrated Tx power, unexpected antenna patterns).

In this paper, we consider combining relative motion capture (i.e. at the body scale) and absolute single-user navigation (i.e. at the building scale) capabilities within heterogeneous WBANs. More particularly, we consider using on-body wireless links in a mesh intra-WBAN topology, as well as off-body wireless links with respect to external elements of infrastructure, set as fixed anchors. Multi-standard wireless on-body nodes are thus required, being compliant with e.g., IR-UWB IEEE 802.15.6 [15] for intra-WBAN communications and IR-UWB IEEE 802.15.4a or IEEE 802.15.4 over larger-range off-body links. The idea is that both on-body and

off-body localization procedures could mutually benefit from each other, while preserving the finest precision of relative localization over large-scale trajectories, contrarily to the first cooperative localization attempt in [16], where the precision of relative localization at the body scale was degraded by the introduction of off-body links. Different options and scenarios are herein compared in terms of location-dependent radio metrics (i.e. TOA, TDOA, RSSI), synchronization constraints and transmission ranges. We also describe a specific 2-step algorithm, which first performs the relative localization of on-body nodes in a body-strapped *Local Coordinates System* (LCS) before applying transformations to express the estimated coordinates into an absolute *Global Coordinates System* (GCS). We also take advantage of the presence of multiple on-body nodes to mitigate body obstructions with respect to external anchors through distance approximations based on neighborhood information. The targeted application will be depicted as *Large Scale Individual Motion Capture* (LSIMC) in the following. Related use cases concern e.g., the live capture of on-field sports gesture, home activity monitoring for non-intrusive and long-term physical rehabilitation.

The paper is structured as follows. In Section II, we introduce the general localization problem. Section III then presents the localization algorithms, as well as the different LSIMC scenarios. In Section IV, we describe a possible enhancement for the mitigation of body obstructions based on graph neighborhood information and distances approximation. Then, Section V accounts for the simulation set-up and parameters, as well as simulation-based results obtained under realistic body mobility. Finally, Section VI concludes the paper.

II. Problem Formulation

We first assume a set of fixed anchor nodes placed at known positions in the indoor environment and forming the building infrastructure. These nodes will be also depicted as *infrastructure anchors* in the following. A second set comprises wireless devices placed on the pedestrian body. These devices can also be classified into two categories, namely simple on-body mobile *nodes* with unknown positions under arbitrary deployment and reference *on-body anchors*. The latter are attached onto the body at known and reproducible positions independently of the body attitude and/or mobility (e.g. on the chest or on the back). A set of such on-body anchors then define a stable Cartesian LCS, which remains unchanged and time-invariant under body mobility.

Fig. 1 shows a typical deployment scenario, where the LCS is obviously in movement and misaligned relatively to an external GCS. In the following, $\{X_i^{ac}\}_{i=1...N_a}$ represents the set of the absolute $3D$ known positions of the N_a fixed infrastructure anchors expressed in the GCS, where N_a should be equal or larger than 4. $\{X_i^a(t)\}_{i=1...n}$ and $\{X_i^r(t)\}_{i=1...n}$ represent respectively the absolute and relative $3D$ unknown positions of the n mobile nodes deployed on the body at time t, as respectively expressed in the GCS and LCS. Similarly, $\{X_i^a(t)\}_{i=n+1...n+m}$ and $\{X_i^r\}_{i=n+1...n+m}$ represent respectively the absolute $3D$ unknown positions of the m

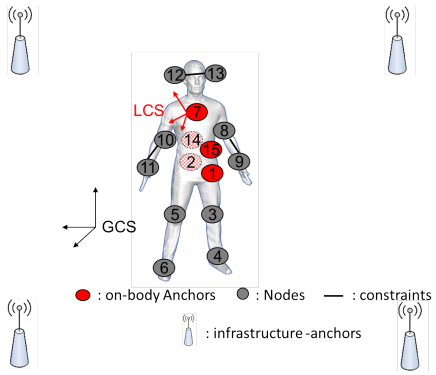

Fig. 1. Typical deployment scenario for the absolute localization of on-body wireless nodes.

on-body anchors at time t and their corresponding relative known positions (time-invariant), where m should be equal or larger than 4. Now let $\widetilde{d}_{ij}(t)$ be one range or pseudo-range measurement available at time t between one on-body node i and a connected node j, j being one on-body node, one on-body anchor or one infrastructure anchor, and let l_{ij} be a constant distance (i.e. time-invariant over body mobility whatever the coordinates system), which will be considered hereafter as a constraint [11].

Given all the available measurements $\{\widetilde{d}_{ij}(t)\}$ at time t, e.g. based on IR-UWB TOA estimation [10] between cooperative on-body devices or between on-body nodes and infrastructure anchors, on the known locations of on-body anchors and infrastructure anchors, the problem that we want to solve consists in estimating the absolute positions of the on-body nodes in the GCS.

III. LSIMC Scenarios and Algorithms

A. 2-Step Approach

1) 1-st Step: The idea here is to start the LSIMC procedure by localizing the on-body nodes relatively to the LCS, using cooperative peer-to-peer range measurements between pairs of devices. Motivated by the possibility to operate under partial connectivity, by latency constraints (i.e. the time elapsed between the collection of the distance measurements and the delivery of location estimates) and by the intrinsic asynchronism potential enabled for nodes' localization, we propose to apply the *Constrained Distributed Weighted Multi-dimensional Scaling* (CDWMDS) algorithm described in [11], which is adapted to relative on-body localization in WBAN. CDWMDS allows each node to localize itself by minimizing a local cost function that depends on its neighborhood information, as follows:

$$\begin{aligned}\hat{X}_i^r(t) \quad = \quad & \underset{X_i^r(t)}{\operatorname{argmin}}\Big[\sum_{j=1,j\neq i}^{n} w_{ij}(t)(\delta_{ij}(t)-\hat{d}_{ij}(X_i^r(t),\hat{X}_j^r(t)))^2 \\ & + \sum_{j=n+1}^{n+m} 2w_{ij}(t)(\delta_{ij}(t)-\hat{d}_{ij}(X_i^r(t),\hat{X}_j^r(t)))^2 \\ & + r_i(t)||X_i^r(t)-\overline{X}_i^r(t)||^2\Big] \end{aligned} \quad (1)$$

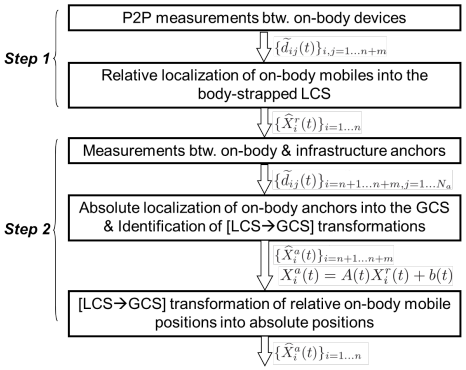

Fig. 2. 2-step LSIMC approach.

where $\hat{X}_i^r(t)$ contains the estimated $3D$ coordinates of node i in LCS available at time t, $\delta_{ij}(t)$ is a so-called observed distance between node i and j at t, $\hat{d}_{ij}(X_i^r(t), \hat{X}_j^r(t))$ denotes the Euclidean distance between nodes i and j, which is built out of estimated coordinates in LCS and equal to $\sqrt{(X_i^r(t) - \hat{X}_j^r(t))^T(X_i^r(t) - \hat{X}_j^r(t))}$, $w_{ij}(t)$ is a weight value, which reflects the connectivity and the accuracy of the range measurements between nodes i and j at time t, $\overline{X}_i^r(t)$ is a vector with prior information about the position occupied by node i at time t, while $r_i(t)$ quantifies the reliability of this prior information.

Two enhancements to the nominal CDWMDS algorithm have been proposed in [11]. The first one consists in using coarse information about the nodes deployment to benefit from geometrical characteristics of the human body. The idea is to introduce fixed links on the body (e.g. links between hand's wrist and elbow) as constraints into the positioning problem. The second improvement consists in taking the latest estimated position available for node i at time $t-1$, as prior information in the local current cost function, using $\overline{X}_i^r(t) = \hat{X}_i^r(t-1)$. The choice accounts for the bounded motion amplitudes of on-body nodes under human mobility. Still relatively to the LCS, this amplitude strongly depends on the node's location itself and hence, we benefit from space-time coherence under body motion and the algorithm's convergence will be faster and easier.

2) 2-nd Step: The second stage consists in converting the relative locations defined into the LCS to absolute locations into the GCS. This transformation of LCS includes a rotation and a translation. Whereas on-body anchors are time-invariant in the LCS under mobility, it is preferable to rely on those nodes to transform the LCS. In $3D$ environments, the absolute locations of at least 4 on-body anchors are needed to find the absolute locations of the other mobile nodes. Hence, we determine the absolute localization of the on-body anchors into the GCS first.

Based on both known on-body ranges and range measurements with respect to external anchors, on-body anchors are localized through non-linear least squares optimization, by minimizing a new local cost function as follows:

$$\hat{X}_i^a(t) = \underset{X_i^a(t)}{\text{argmin}}[\sum_{j=n+1,j\neq i}^{n+m} w_{ij}(t)(d_{ij}(t) - \hat{d}_{ij}(X_i^a(t), \hat{X}_j^a(t)))^2 + \sum_{k=1}^{N_a} w_{ik}(t)(\delta_{ik}(t) - \hat{d}_{ik}(X_i^a(t), X_k^{ac}))^2] \quad (2)$$

where $\hat{X}_i^a(t)$ is the vector of the estimated $3D$ coordinates of on-body anchor i into the GCS at time t, $d_{ij}(t)$ and $\hat{d}_{ij}(X_i^a(t), \hat{X}_j^a(t))$ denotes respectively the true distance between on-body anchors i and j and the corresponding distance built out of the estimated coordinates, N_a is the number of infrastructure anchors and $\delta_{ik}(t)$ is the observed distance between on-body anchor i and infrastructure anchor k.

Getting back to our initial aim of localizing on-body nodes into the GCS, the absolute coordinates can be obtained out of the relative coordinates into the LCS after a few transformations (i.e. rotation and a translation), which can be represented as follows:

$$X_i^a(t) = A(t)X_i^r(t) + b(t) \quad (3)$$

The goal now is to estimate the rotation matrix A and the translation component b out of noisy observations, by minimizing the difference in the least squares sense between the absolute locations of on-body anchors and the corresponding versions, which are obtained through the transformation of estimated relative positions. For a given on-body anchor l, we set $\Delta X^r(t) = [\Delta X_{n+1}^r(t), ..., \Delta X_{l-1}^r(t), \Delta X_{l+1}^r(t), ..., \Delta X_{n+m}^r]$ and $\Delta X^a(t) = [\Delta X_{n+1}^a(t), ..., \Delta X_{l-1}^a(t), \Delta X_{l+1}^a(t), ..., \Delta X_{n+m}^a]$, where $\Delta X_i^r(t) = X_i^r(t) - X_l^r(t)$ and $\Delta X_i^a(t) = X_i^a(t) - X_l^a(t)$ for $l \neq i$. The alignment problem can therefore be formulated as a least-squares optimization problem, as follows:

$$\hat{A}(t) = \underset{A(t)}{\text{argmin}} \sum_{i=n+1,i\neq k}^{n+m} ||A(t)\Delta X_i^r(t) - \Delta X_i^a(t)||^2 \quad (4)$$

The analytical solution of this linear least-squares problem is given by $\hat{A}(t) = \Delta X^a(t)(\Delta X^r(t))^T(\Delta X^r(t)(\Delta X^r(t))^T)^{-1}$. Finally, the absolute locations of all the on-body mobile nodes in the GCS are derived from their corresponding relative versions in the LCS, as follows:

$$\hat{X}_i^a(t) = \hat{A}(t)(\hat{X}_i^r(t) - \hat{X}_l^r(t)) + \hat{X}_l^a(t) \quad (5)$$

B. Single-Step Approach

The idea here is to compute directly the positions of on-body mobile nodes in the GCS, by combining simultaneously all the available measurements, which can be performed between on-body devices or with respect to infrastructure anchors. Accordingly, the cost function to be minimized by each on-body device i is rather similar to that of equation (2) but now

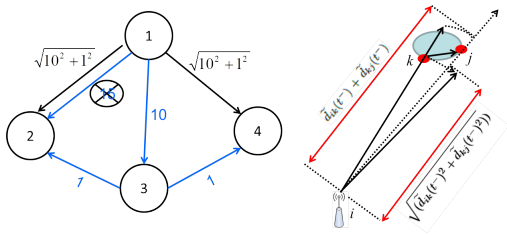

Fig. 3. Example of distance estimation over neighborhood graph (left): the blue graph represents the initial graph based on the observation distances and connectivity information. The black graph is reconstructed based on the calculation of the shortest paths. Example of reconstructed distance through triangular and linear estimation over off-body links (right).

incorporates also cooperative distance measurements between on-body devices, as follows:

$$\hat{X}_i^a(t) = \underset{X_i^a(t)}{\text{argmin}}[\sum_{j=1,j\neq i}^{n+m} w_{ij}(t)(\delta_{ij}(t) - \hat{d}_{ij}(X_i^a(t), \hat{X}_j^a(t)))^2 + \sum_{k=1}^{N_a} w_{ik}(t)(\delta_{ik}(t) - \hat{d}_{ik}(X_i^a(t), X_k^{ac}))^2] \quad (6)$$

IV. Distances Estimation over Neighborhood Graph

A graph is usually considered as a collection of vertices (or nodes) and edges (or distances) that connect pairs of vertices. In the very WBAN localization context, we assume that the on-body devices and infrastructure anchors form such a graph. The edges, which can be weighted by the observation distances, then reflect connectivity between the different entities.

So as to mitigate link obstructions, as an improvement of the previous algorithms described in Section III, we propose to reconstruct the graph based on connectivity and measurement information, by computing the shortest distances over neighborhood graph. The idea is to start by initializing the weight of an edge between nodes i and j by the observation distance $\widetilde{d}_{ij}(t)$ in case of connectivity, and by ∞ otherwise. In a second step, we replace each weight (i.e. distance) by the shortest path separating the graph nodes in the local neighborhood by updating $\widetilde{d}_{ij}(t^+) = min(\widetilde{d}_{ij}(t^-), \sqrt{(\widetilde{d}_{ik}(t^-)^2 + \widetilde{d}_{kj}(t^-)^2}$. The selection of a triangular estimator (i.e. $\sqrt{(\widetilde{d}_{ik}(t^-)^2 + \widetilde{d}_{kj}(t^-)^2)}$) instead of the linear one (i.e. $\widetilde{d}_{ik}(t^-) + \widetilde{d}_{kj}(t^-)$), appears more adaptable to the deployment of on-body devices (i.e. 2 on-body devices and an infrastructure anchor are most likely not aligned but form a triangle). Fig. 3 shows an example for a graph having 4 nodes, with the initial graph exhibiting a disconnection between node 1 and 4 and its reconstructed version based on the shortest observed path. Our proposal, which performs distance estimation over neighborhood graph, generally leads to an important reduction of the ranging errors affecting the measured distances (e.g. outliers), and more noticeably in *Non Line Of Sight* (NLOS) conditions. Moreover, missing distances under partial connectivity are approximated whenever one path has been found.

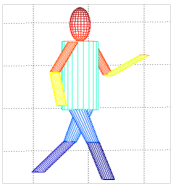

Fig. 4. Biomechanical mobility model based on a piece-wise cylindrical representation, used in the generation of realistic inter-node distance measurements under body mobility.

V. Simulations and Results

A. Scenario Description

In our evaluation framework, human mobility is based on a mixed model, like in [17]. A macroscopic model accounts for the body center mobility, where the reference point follows a Random Gauss Markov process [16]. This model is couled with a biomechanical cylindrical-based model. Body extremities are modeled as articulated objects, which consist of rigid cylinders connected to each other by joints. A snapshot of the resulting articulated body under pedestrian mobility is represented in Fig. 4 at an arbitrary time stamp. This biomechanical model enables the generation of true inter-node distances between on-body nodes, whatever the time stamp.

In our scenario, for each new random realization, the reference body moves in a $20m \times 20m \times 4m$ $3D$ environment with a constant speed of $1m/sec$ for $80sec$. The scene is surrounded by 8 infrastructure anchors set at the corners. The network deployment is similar to that presented on Fig. 1, with 5 on-body anchors and 10 blind on-body nodes.

B. Simulation Parameters

Concerning the physical radio parameters, we differentiate intra-WBAN and off-body links. We first assume IR-UWB on-body radio links, as recently promoted by the IEEE 802.15.6 standard [15]. We also consider that the received power is larger than the receiver sensitivity, which allows peer-to-peer communications with a worst-case *Packet Error Rate* (PER) of 1%, as specified by the standard. This PER figure is applied to each single packet involved in 3-way ranging protocol transactions within a time division multiple access scheme [17], thus emulating uncomplete ranging transactions (i.e. whenever at least one packet is lost out of 3). Moreover, based on the TOA-based IR-UWB model in [10], which has been specified in the IEEE 802.15.6 mandatory band centered around $4GHz$ with a bandwidth of $500MHz$, random ranging errors are added to measurements at time stamp t depending on the current LOS or NLOS channel configuration, as follows:

$$\begin{aligned} \widetilde{d}_{ij}(t) &= d_{ij}(t) + n_{ij}(t) && if\ LOS \\ \widetilde{d}_{ij}(t) &= d_{ij}(t) + n_{ij}(t) + b_{ij}(t) && if\ NLOS \end{aligned} \quad (7)$$

where $\widetilde{d}_{ij}(t)$ and $d_{ij}(t)$ are respectively the measured and real distances between nodes i and j at time t, $n_{ij}(t)$ is a

LOS	NLOS
σ_n=0.3 m	σ_n=0.5 m
$b_{ij}(t) = 0$	$b_{ij}(t) \in$ [1, 2] m

TABLE I
TOA-BASED RANGING ERROR PARAMETERS OVER INDOOR OFF-BODY IR-UWB LINKS, ACCORDING TO [16].

	LOS		NLOS	
	n	PL_0	n	PL_0
Rx heart	-2	-38.92 dB	-0.4	-62.62 dB
Rx left hip	-2	-51.94 dB	-0.1	-68.78 dB

TABLE II
RSSI MODEL PARAMETERS OVER INDOOR OFF-BODY NB LINKS AT 2.45 GHZ, ACCORDING TO [18].

centered Gaussian random variable with standard deviation σ_n and $b_{ij}(t)$ is a bias term due to the absence of direct path when estimating TOA.

Simplifying the model from [10], our simulations are carried out using a constant σ_n equal to $10\,cm$, independently of the instantaneous signal to noise ratio, but still in the range of values observed in [10] based on real measurements. $b_{ij}(t)$ is a random positive bias added only into NLOS conditions, which follows a uniform distribution in $[0\,10]cm$. Moreover, $b_{ij}(t)$ is assumed constant over one walk cycle in first approximation (i.e. $b_{ij}(t) = b_{ij}, \forall t$), which is also in compliance with first empirical observations from [10] with dynamic links over NLOS portions (i.e. reproducible bias from one walk cycle to the next).

As for off-body links between on-body devices and infrastructure anchors, radiolocation measurements can be delivered through IR-UWB TOA or NB RSSI estimation. In case of IR-UWB (e.g. according to the IEEE 802.15.4a standard), the conditional TOA-based ranging error model is similar to that of equation (7), but noise parameters have been adjusted according to [16], as reported in table I. NLOS conditions are assumed to be caused uniquely by body shadowing here. Regarding NB RSSI-based ranging (e.g. according to the IEEE 802.15.4a standard in the band centered around 2.4GHz), inspired by the off-body channel model in [18], which has been specified in the ISM band (i.e. at 2.45 GHz), the path-loss model used in our simulations is simplified by eliminating fast fading components (i.e. considering that one would average over a sufficient number of consecutive RSSI readings per link in a real system), as follows:

$$PL(d) = PL_0 + 10nlog_{10}(d/d_0) + S \tag{8}$$

where $PL(d)$ is the path-loss in dB between two devices separated by a distance d, PL_0 represents the path-loss in dB at a reference distance $d_0 = 1\ m$, n is the path-loss exponents and S represents the body shadowing.

Simplifying further, we also suppose that S is normally distributed with zero mean and standard deviation $\sigma_S = 2$ dB. Table II summarizes the parameters from [18] for WBAN planar monopole antennas and two different specific links. Note that the RSSI radiolocation metrics will be integrated only in the 2-step localization scenario, where the infrastructure anchors are just connected to on-body anchors. We have classified those links into two different sets depending on the locations of their involved on-body nodes. Generalizing the model in [18], the two sets of links are thus associated with the same channel parameters as that observed for an antenna placed either on the heart or on the left hip. The estimated distance is finally extracted from RSSI readings using the maximum-likelihood estimator proposed in [19], as follows:

$$\widetilde{d}_{ij}(t) = exp(M_{ij} - L_{ij}^2) \tag{9}$$

where $M_{ij} = \frac{\sigma_S ln(10)}{10n_{ij}}$ and $L_{ij} = \frac{(PL_{ij} - PL_0)ln(10)}{10n_{ij}} + ln(d_0)$. Finally, concerning the localization algorithm setting, three fixed-length link constraints are imposed to the CDWMDS algorithm a priori like in [11], as materialized with black lines in Fig. 1. We also set $w_{ij}(t) = 1$ in connectivity conditions and 0 otherwise, regardless to neighbor's information reliability (i.e. with no soft weighting under connectivity). $r_i(t)$ is also equal to 1 for simplifications. Finally, localization updates are realized in average with a refreshment rate of 30 ms.

C. Simulation Results

Based on the previous models and settings, simulations have been carried out to illustrate and compare the LSIMC performances of both single- and 2-step localization approaches. We have also considered several options for off-body links (in the latter 2-step embodiment), integrating different radiolocation metrics, namely TOA, TDOA and RSSI. Moreover, additional simulations aim at illustrating the benefits from estimating the distances over neighborhood graph in order to mitigate obstructions and too large measurement errors. Running trials of the walk cycle with 100 independent realizations of measurement error processes, the *Root Mean Squared Error* (RMSE) has been characterized for each on-body mobile node.

As shown on Fig. 5, mostly due to severe obstructions and partial connectivity conditions, the performances of the standard 2-step RSSI-based and 1-step TOA-based approaches look rather poor and definitely not compliant with the requested LSIMC level of precision, even if the TOA-based option seems slightly better. However, based on IR-UWB TOA estimation over off-body links (i.e. TOA or TDOA) in the 2-step approach, rather clear gains can already be observed in comparison with the single-step approach, even though the resulting average precision would be mostly interesting to navigation application and still meaningless for LSIMC, with an average RMSE over all the on-body nodes respectively equal to 1.1 m and 1.2 m using the TOA and TDOA metrics over off-body links, hence justifying further enhancements.

On Fig 6, we show similar results with the additional distance estimation technique, which consists in identifying the shortest distance over neighborhood graph. The average RMSE per node is then decreased from 1.1 m down to 0.31 m, leading to a significant improvement by 72 %. On the one hand,

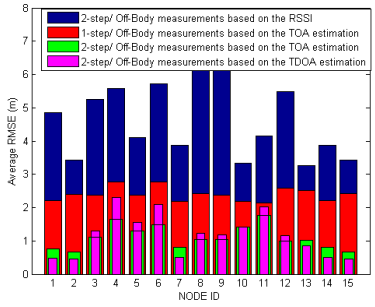

Fig. 5. RMSE of estimated locations per on-body node (ID) with both single- and two-step LSIMC based on TOA, TDOA and RSSI metrics over off-body links.

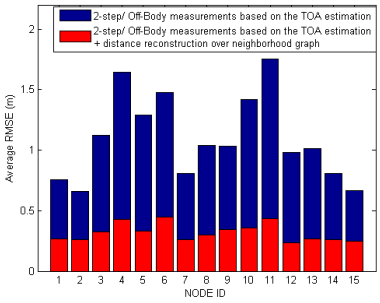

Fig. 6. RMSE of estimated locations per on-body node (ID) with two-step LSIMC based on TOA metrics over off-body links and distances estimation over neighborhood graph.

comparable levels of precision are now achieved for absolute on-body localization at the building scale in comparison with the best performance of relative on-body localization at the body-scale [11]. On the other hand, penalized nodes located at the body extremities, which classically suffer from lower connectivity, poor geometric dilution of precision and higher accelerations (e.g. nodes 4, 6, 9 and 11 in our example), now seem to enjoy better robustness in comparison with other nodes. Considering relaxed deployment constraints and the claimed WBAN low consumption, these results could make this LSIMC solution a reasonable alternative to costly, power greedy and geographically restricted technologies.

VI. Conclusion

In this paper, we have jointly addressed the problems of motion capture and navigation over large-scale indoor trajectories in location-enabled heterogeneous wireless body area networks. Two approaches have been presented to estimate the absolute locations of on-body nodes in a global coordinates system, considering different radiolocation metrics over off-body links with respect to infrastructure anchors. One 2-step solution relies on preliminary relative localization at the body scale and applies further transformations through the absolute localization of on-body anchors. Finally, we have proposed an algorithm that estimates the shortest path between on-body and infrastructure anchors over neighborhood graph to compensate for radio obstructions and large measurement errors. Future works will concern cooperative navigation in groups of WBANs and field experiments based on real on-body IR-UWB nodes.

Acknowledgment

This work has been carried out in the frame of the *COR-MORAN* project (ANR11-INFR010), which is funded by the *French National Research Agency* (ANR).

References

[1] T.B. Moeslund, A. Hilton, and V. Krager, "A Survey of Advances in Vision-based Human Motion Capture and Analysis", Computer Vision and Image Understanding, Special Issue on Modeling People - Vision-based understanding of a persons shape, appearance, movement and behaviour, vol. 104, is. 2-3, pp. 90-126, Nov.-Dec. 2006

[2] http://www.codamotion.com/

[3] J.F. OBrien, R.E. Bodenheimer, G.J. Brostow, and J.K. Hodgins, "Automatic Joint Parameter Estimation from Magnetic Motion Capture Data," in Proc. Graphics Interface Conf., 2000.

[4] T. Sakaguchi, T. Kanamori, H. Katayose, K. Sato, and S. Inokuchi. "Human motion capture by integrating gyroscopes and accelerometers," in Proc. IEEE/SICE/RSJ MFI96, 1996.

[5] A. Andreadis, A. Hemery, A. Antonakakis, G. Gourdoglou, P. Mauridis, D. Christopoulos, and J. Karigiannis, "Real-time Motion Capture Technology on a Live Theatrical Performance with Computer Generated Scenery," in Proc. PCI'10, 2010

[6] J.D. Hol, F. Dijkstra, H. Luinge, and T.B. Schöny, "Tightly Coupled UWB/IMU Pose Estimation," in Proc. IEEE ICUWB09, pp. 688692, Vancouver, Sept. 2009

[7] D. Vlasic, R. Adelsberger, G. Vannucci, J. Barnwell, M. Gross, W. Matusik, and J. Popovic, "Practical Motion Capture in Everyday Surroundings", ACM Trans. Graph., 26, 2007.

[8] H.A. Shaban, M.A. El-Nasr, R.M. Buehrer, "Toward a Highly Accurate Ambulatory System for Clinical Gait Analysis via UWB Radios," IEEE Trans. on Information Technology in Biomedicine, vol.14, no.2, pp.284-291, March 2010.

[9] Z.W. Mekonnen, E. Slottke, H. Luecken, C. Steiner, and A. Wittneben, "Constrained maximum likelihood positioning for UWB based human motion tracking," in Proc. IPIN'10, pp.1-10, Sept. 2010.

[10] J. Hamie, B. Denis, R. D'Errico, C. Richard, "Modeling of Intra-BAN Ranging Errors Based on IR-UWB TOA Estimation," in Proc. BodyNets'12, Oslo, Oct. 2012.

[11] J. Hamie, B. Denis, C. Richard, "Nodes Updates Censoring and Scheduling in Constrained Decentralized Positioning for Large-Scale Motion Capture based on Wireless Body Area Networks," in Proc. BodyNets'12, Oslo, Oct. 2012.

[12] M. Mhedhbi, M. Laaraiedh, and Bernard Uguen, "Constrained LMDS Technique for Human Motion and Gesture Estimation," in Proc. WPNC'12, March 2012

[13] Y. Gu, A. Lo, I. Niemegeers, "A Survey of Indoor Positioning Systems for Wireless Personal Networks," IEEE Communications Survey & Tutorals, vol. 11, no. 1, 2009

[14] J. Youssef, B. Denis, C. Godin, S. Lesecq, "Pedestrian Tracking Solution Combining an Impulse Radio Handset Transmitter with an Ankle-Mounted Inertial Measurement Unit," International Journal of Navigation and Observation (IJNO), Hindawi Publishing Corporation, 2012

[15] K.S. Kwal, S. Ullah, N. Ullah, "An Overview of IEEE802.15.6 standard", in Proc. ISABEL'10, Nov. 2010.

[16] E. Ben Hamida, M. Maman, B. Denis, and L. Ouvry, "Localization Performance in Wireless Body Sensor Networks with Beacon Enabled MAC and Space-time Dependent Channel Model," in Proc. IEEE PIMRC'10, pp.128-133, Sept. 2010.

[17] M. Maman, F. Dehmas, R. D'Errico, and L. Ouvry, "Evaluating a TDMA MAC for Body Area Networks Using a Space-time Dependent Channel Model," in Proc. IEEE PIMRC'09, Sept. 2009.

[18] R. Rosini, R. D'Errico, "Off-Body Channel Modelling at 2.45 GHz for two Different Antennas," in Proc. EUCAP'12, pp.3378-3382, March 2012.

[19] M. Laaraiedh, S. Avrillon, B. Uguen, "Enhancing Positioning Accuracy through Direct Position Estimators Based on Hybrid RSS Data Fusion," in Proc. IEEE VTC-Spring'09, pp.1-5, April 2009.